A STUDY ON UNSTABLE DUCTILE FRACTURE

S. Aihara*, S. Machida* and T. Kanazawa*

*Dept. of Naval Architecture, Univ. of Tokyo,
7-3-1, Hongo, Bunkyo-ku, Tokyo, Japan

ABSTRACT

This paper discusses criteria on stable crack growth and unstable ductile fracture in terms of J-integral R curve and crack tip opening angle (CTOA) R curve. In order to verify the proposed criteria, three point bend tests and deep notch tests were carried out. Stable crack growth tests indicated that J R curve and CTOA R curve were almost independent of initial crack length. On the other hand, the tests with highly compliant loading systems showed that the initiation of unstable ductile fracture compared well with the predicted instability point.

KEYWORDS

Ductile fracture; crack propagation; unstable ductile fracture; R curve; J-integral; crack tip opening angle.

INTRODUCTION

The assessment of unstable ductile fracture is indispensable in some structure such as piping in nuclear power plant, where stress corrosion cracking has been found and structural integrity against severing of pipes by tearing instability is strongly to be assured. In order to prevent unstable ductile fracture, suitable material selection and design procedure are needed. Unstable ductile fracture itself, however, has not been fully understood yet.

Recently, it has become common to characterize ductile crack growth using J-integral, crack tip opening displacement and angle, and other fracture parameters (Hutchinson and Paris, 1979; Paris and others, 1979; Rice and others, 1979; Shih and others, 1979). However, the investagations into instability criteria and their experimental verifications are rather limited (Kanazawa, 1979; Paris and others, 1979b). In this paper, ductile instability criteria in terms of J-integral and crack tip opening angle are investigated and their validity is discussed on the basis of experiments and numerical analysis.

CRITERIA ON CRACK GROWTH AND INSTABILITY

A Criterion Based on J Resistance Curve

The instability criterion in terms of J Resistance curve (J R curve) can be stated in the following manner. Imagine a body with a crack which grows stably with the increase in applied load or displacement. Assuming infinitesimal growth of the crack under fixed grip condition, the rate of change in applied J during infinitesimal crack growth is compared with the slope of J R curve. Instability commences when the rate of change in applied J exceeds the slope of J R curve, namely

$$\frac{dJ^{F.G.}}{da} \geq \frac{dJ_R}{da} \tag{1}$$

$dJ^{F.G.}/da$ is strongly dependent of the compliance of loading system and specimen configuration, namely it increases with the increase of the compliance of a structural component under consideration. Therefore, instability is liable to take place under highly compliant system.

$dJ^{F.G.}/da$ can be obtained by considering the change in applied J value during infinitesimal crack growth and applied displacement and fixed grip condition. The results for deeply cracked bend speicmen is expressed by

$$\frac{dJ^{F.G.}}{da} = \frac{64B(W-a)^2}{L^2} f^2 \left\{\frac{1}{C_{nc}} + \frac{16B(W-a)^2}{L^2}\frac{df}{d\theta_c}\right\}^{-1} - \frac{J}{W-a} \tag{2}$$

where B,W,L and "a" are thickness, depth, bending span and crack length respectively, C_{nc} is the elastic compliance corresponding to the displacement of no crack component including that of loading system if necessary, f is a function of rotational angle due to crack, θ_c. Also, $dJ^{F.G.}/da$ for deeply cracked plate in tension is expressed by

$$\frac{dJ^{F.G.}}{da} = \frac{1}{(1+CB\sigma_N')}\left(CB\sigma_N + \frac{\Delta_p}{W-2a} - B\frac{\partial g}{\partial P}\Big|_a\right)\left(2\sigma_N + B\sigma_N'\frac{\partial g}{\partial P}\Big|_a - \frac{2\sigma_N'}{W-2a}\Delta_p\right)$$
$$- B\sigma_N\frac{\partial g}{\partial P}\Big|_a + \frac{\partial g}{\partial a}\Big|_P - \frac{2}{W-2a}(J-g), \tag{3}$$

where B, W, a are thickness, width and crack length of a specimen, C is the elastic compliance of specimen and loading system, P is applied load, σ_N is net section stress and prime denotes a derivative with respect to $\Delta_p/(W-2a)$, Δ_p is plastic component of load point displacement, g is the linear elastic energy release rate. Eqs. (2) and (3) are essentially equivalent to those obtained by Hutchinson and Paris (1979).

A Criterion Based on Crack Tip Opening Angle R curve

Recently, crack tip opening angle (CTOA) has been found to be an attractive parameter characterizing stable crack growth from finite element analyses. (Kanninen and others,1979; Shih and others, 1979). However, instability criterion based on CTOA has not been well established yet. In this paper, unstable fracture is assumed to take place when the applied CTOA under fixed grip condition, $(CTOA)^{F.G.}$, exceeds the CTOA of material resistance, $(CTOA)_R$. Analogously to the J based criterion, the instability condition is expressed by

$$(CTOA)^{F.G.} \geq (CTOA)_R \tag{4}$$

$(CTOA)^{F.G.}$ is dependent of the configuration of cracked body and the compliance of loading system.

Rice and others (1979) have presented the asymptotic solution of the deformation field near crack tip which grows steadily through elastic-perfectly plastic material under well contained plane strain condition. Crack opening profile near crack tip can be obtained as follows.

$$\delta = r\omega\frac{dq}{da} + \beta\frac{\sigma_0}{E} r \ln\left(\frac{eR}{r}\right), \quad \text{as } r \to 0, \tag{5}$$

where r is the distance from crack tip, ω is a function of the configuration of a specimen, q is load point displacement, β is 5.08 for Poisson's ratio 0.3, σ_0 and E are flow stress and Young's modulus, respectively, e is the natural logarithm base, R is nearly equal to plastic zone size for small scale yielding and the order of uncracked ligament size for full yielding. Crack tip opening angle can not be defined definitely because the angle at the crack tip is π. So, we define the crack tip opening angle as the opening displacement at $r=r_m$ devided by r_m, where r_m is some small distance equivalent to fracture process zone size. CTOA thus defined should not be regarded as "physical" crack tip opening angle, but rather be regarded as "virtual" crack tip opening angle which represents the intensity of deformation near the crack tip. In the case of a bend specimen, rotational angle of crack component θc can be adopted as q, and considering the deformation of a bend specimen with a stationary crack, CTOA can be expressed as

$$CTOA = kb\frac{d\theta c}{da} + \beta\frac{\sigma_0}{E}\ln\left(\frac{eR}{r_m}\right), \tag{6}$$

where b is the uncracked ligament size, and k is the rotational factor which has the value 0.37 from slip line theory. On the other hand, $(CTOA)^{F.G.}$ can be obtained by considering the rate of θ_c during infiniteismal crack growth under fixed grip condition. The result is expressed by

$$(CTOA)^{F.G.} = k\frac{32Bb^2}{L} f(\theta_c)\left\{\frac{1}{C_{nc}} + \frac{16Bb^2}{L^2}\frac{df}{d\theta_c}\right\}^{-1} + \beta\frac{\sigma_0}{E}\ln\left(\frac{eR}{r_m}\right). \tag{7}$$

In the case of a deeply cracked plate in tension, CTOA is expressed by

$$CTOA = k'\frac{d\Delta}{da}P + \frac{\sigma_0}{E}\ln\left(\frac{eR}{r_m}\right), \tag{8}$$

where factor k' approximately takes the value 2 for fully yielded double edge cracked plate from slip line theory. $(CTOA)^{F.G.}$ can be obtained as follows,

$$(CTOA)^{F.G.} = \frac{2CB}{(1+CB\sigma_N')}\left\{2\sigma_N - \frac{1}{C}\frac{\partial g}{\partial P}\Big|_a - \frac{2\sigma_N'\Delta P}{W-2a}\right\} + \beta\frac{\sigma_0}{E}\ln\left(\frac{eR}{r_m}\right). \tag{9}$$

J based and CTOA based instability criteria, eqs. (1) and (4), is fundamentally equivalent to estimate the point where the curve of load versus load point displacement including that of loading system starts to fall down vertically, in other words, crack propagates without increasing further displacement.

EXPERIMENTAL PROCEDURE

In order to verify the validity of the instability criteria stated above, we carried out small scale three point bend tests and large scale double edge deep notch tests.

The material tested is 11 mm thick mild steel with yield strength 294 MPa and tensile strength 432 MPa at room temperature.

In order to establish J and CTOA R curves, it is necessary to determine experimentally ductile crack length as a function of load point displacement. For bend specimens, ductile crack length was determined by elastic unloading compliance technique and by visual as well as photographic observations for deep notch test. The functions $f(\theta_c)$ in eq.(2) and σ_N $(\Delta p/(w-2a))$ in eq.(3) were also determined experimentally and were fitted to polynomials, which were found to be relatively independent of initial crack lengths and of whether ductile crack grew or not. Then, J and CTOA R curve could be estimated.

In the case of unstable fracture tests, load was applied to specimens through compliant setup, namely, spring bars for bend tests and pipe tabs for deep notch tests, which are shown in Fig. 1.

RESULTS AND DISCUSSION

J Based Fracture Criterion

Figure (2) shows the J R curves estimated from the results of conventional bend tests (without compliant loading system) for different initial crack length at room temperature. Though small differences in J R curves for different initial crack length exist, any systematic trend with respect to initial crack length can not be observed. Therefore, J R curve can be considered approximately as a characteristic curve which describes the material resistance property against ductile crack growth. In the Figure, J R curve calcultaed by finite element crack growth simulation is also presented for crack to width ratio 0.5. It is seen that the experimental J which is based on deformation theory and the finite element J which is based on line integral passing through far field have not any difference. J R curves for deep notch tests were also estimated and found to be independent of temperature, if devided by flow stress at each temperature.

J R curves of bend and deep notch tests can not be compared each other, because the mode of fracture was different, namely, nearly flat fracture with shear lips for bend specimens and slat fracture except the initial stage of crack growth for deep notch tests.

Unstable fracture tests were carried out with various combination of initial crack length and compliance of loading system. Figure (3) shows the change in dJ_R/da and $dJ^{F.G.}/da$, normalized by E/σ^2 and plotted against rotational angle due to crack θ_c, for bend specimens of the crack to width ratio 0.5 with three degrees of compliance. In the case of test without spring bars (conventional test) and with low compliant spring bars, ductile crack propagated stably throughout the deformation. On the other hand, in the case of the test with highly compliant spring bars, crack growth changed from stable to unstable manner. It is seen that the greater the compliance and the smaller the crack to width ratio is, the more liable the instability is to take place. Figure 4 shows the test results of deep notch tests. $dJ^{F.G.}/da$ of the test without pipe tabs was nearly zero throughout the test and the crack propagated stably, on the other hand, $dJ^{F.G.}/da$ of tests with pipe tabs (two degrees of compliance) increased with the increase of deformation and intersected dJ_R/da curve.

CTOA Based Fracture Criterion

Figure 5 shows the CTOA R curve of bend specimens with various crack length. It is seen from the figure that the CTOA decreased drastically in the initial part of crack growth and is saturated to constant value of 0.2 radian.

In order to verity the validity of eq.(6), finite element analysis was carried out. In the analysis, the amount of crack growth for given load point displacement was determined from experimental data. Crack growth was modeled by the nodal force relaxation technique. The element size along crack path is 0.25 mm, 1.25% of uncracked ligament size.

Figure 6 shows the comparison of CTOA's estimated by eq.(6) and by finite element analysis. In the figure, crack opening angle (COA) defined by original crack tip was also plotted. It is seen that finite element CTOA R curve lies within the

scatter band of experimental CTOA R curve, therefore the CTOA estimation formula, eq.(6), seems to be valid. Whereas the value of COA differs from that of CTOA and could possibly be influenced by specimen configuration, thus has no meaning as a material property.

An important aspect in Fig. 5 is that the CTOA R curve is almost independent of uncracked ligament size, which suggests that the CTOA R curve is unique under the same mode of fracture and constraint.and that ductile fracture can be characterized by CTOA R curve.

CTOA R curves were also estimated at sub zero temperatures (-20 ∿ -73°C) and were found to be fairly independent of temperature within the range tested.

Figure 7 shows the result of deep notch test. Despite the modes of fracture were different for bend and deep notch specimen, the saturated value of CTOA was nearly the same.

Figures 8 (a), (b) and (c) show the change in $(CTOA)_R$ and $(CTOA)^{F.G.}$ plotted against θ_c for bend tests. In the Figures, the experimental transition range from stable to unstable fracture is also indicated. It is seen that the predicted instability point (the intersection of each curve) compares well with the test results. The trends of $(CTOA)^{F.G.}$ curves in the Figures were found to agree well with those by finite element simulation, thus eq.(7) is proved to be valied.

Figure 9 shows the results of deep notch test and the same conclusion is obtained as in the bend tests.

CONCLUSIONS

It was found that J R curve and CTOA R curve are almost independent of size of specimen if the mode of fracture and constraint is the same and can be characterized as the material resistance property against ductile crack growth. The estimation procedure of CTOA R curve is rather simple and seems to be relevant. However, the limitations for using J and CTOA R curve should be established.

The instability can be predicted by the theory presented in this paper with reasonable accuracy.

The application of the present theory to more complicated problems for example, to the assessment of the cracks in nuclear power plant pipings, is a future subject, which needs some extensions and modifications of the present method.

ACKNOWLEDGEMENT

Part of the experiments were carried out at Nippon Steel Products R.&D. Laboratory. We would like to thank Dr. H. Mimura, Mr. M. Ogasawara and Mr. Y. Kuriyama. We also thank Mr. A. Inami, Sumitomo Metal Co., for his co-operation for the experiments and analysis.

REFERENCES

Hutchinson, J. W., and Paris, P. C. (1979). Instability of the tearing mode of elastic-plastic crack growth. ASTM STP 668, 37 - 64.

Kanazawa, T., Machida, S., and Aihara, S. (1979). Unstable fracture from stable fibrous crack growth. J. Soc. Naval Architects of Japan, 146, 474 - 480.

Kanninen, M. F., Rybicki, E. F., Stonesifer, R. B., and Broek, D. (1979). Elastic-plastic fracture mechanics for two-dimensional stable crack growth and instability problems. ASTM STP 668, 121 - 150.

Paris, P.C., Tada, H., Zahoor, Z., and Ernst, H. (1979a). Instability of the tearing mode of elastic-plastic crack growth. ASTM STP 668, 5 - 36.

Paris, P.C., Tada, H., Zahoor, A., and Ernst, H. (1979b) An initial experimental investigation of the tearing instability. ASTM STP 668, 251 - 265.

Rice, J. R., Drugan, W. J., and Sham, T. L. (1979). Elastic plastic analysis of growing cracks. COO - 3084/65, Brown Univ.

Shih,C. F., DeLorenzi, H. G., and Andrews, W. R. (1979). Studies on crack initiation and stable crack growth. ASTM STP668, 65 - 120.

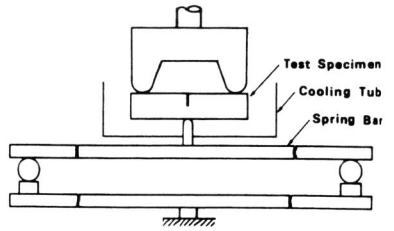

Spring Bar			Test Specimen	
	Span, mm	Compliance, mm/kg	W	40 mm
I.	830	7.25×10^{-3}	L	160
II.	1340	3.16×10^{-2}	B	11

Fig. 1(a) Testing set up with bend specimen.

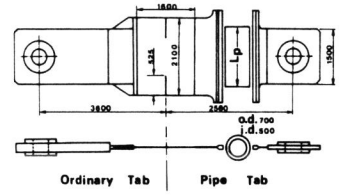

Tab		Lp	Compliance	Test Specimen	
Pipe Tab	I.	1615mm	9.1×10^{-5} mm/kg	W	2100 mm
	II.	2500	7.1×10^{-5}	a	525
Ordinary Tab	–	–	3.6×10^{-6}	B	11

Fig. 1(b) Testing set up with deep notch specimen.

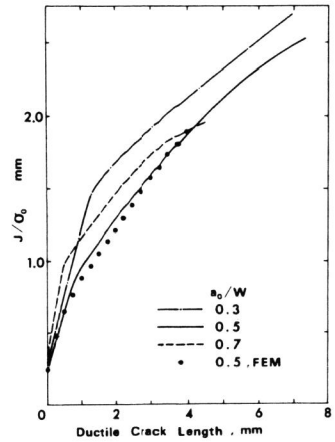

Fig. 2 J R curve for bend specimen.

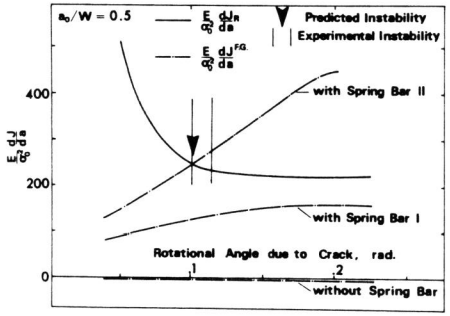

Fig. 3 Comparison of $dJ^{F.G.}/da$ and dJ_R/da for deep specimen.

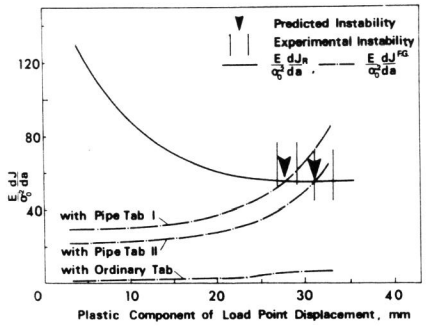

Fig. 4 Comparison of $dJ^{F.G.}/da$ and dJ_R/da for deep notch test.

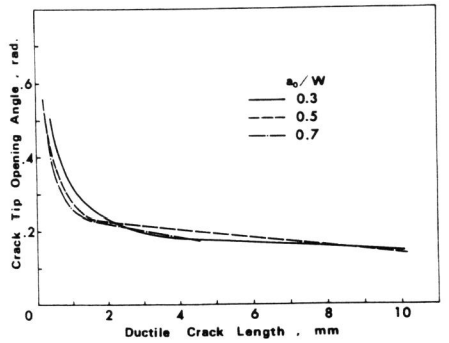

Fig. 5 CTOA R curve for bend specimen.

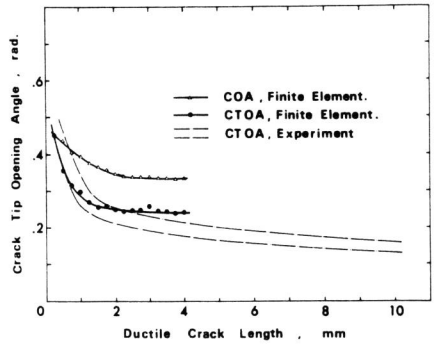

Fig. 6 CTOA R curve from finite element analysis.

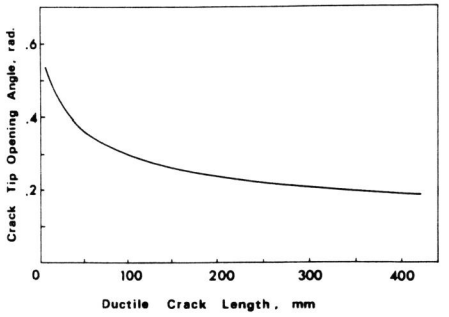

Fig. 7 CTOA R curve for deep notch test.

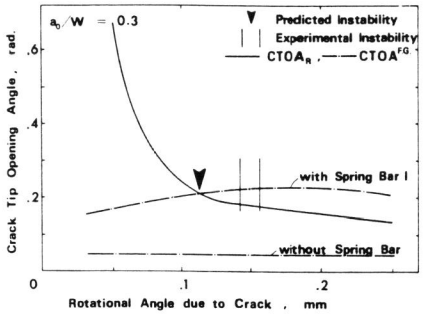

Fig. 8(a) Comparison of $(CTOA)^{F.G.}$ and $(CTOA)_R$ for bend specimen.

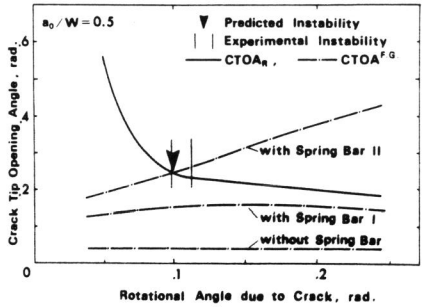

Fig. 8(b) Comparison of $(CTOA)^{F.G.}$ and $(CTOA)_R$ for bend specimen.

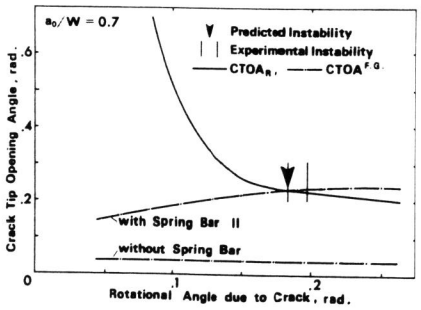

Fig. 8(c) Comparison of $(CTOA)^{F.G.}$ and $(CTOA)_R$ for bend specimen.

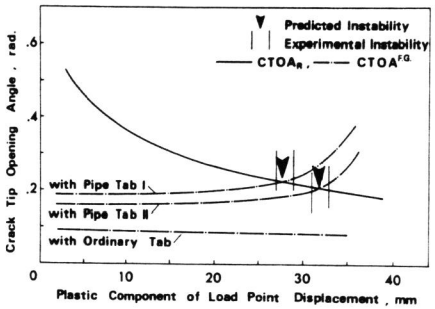

Fig. 9 Comparison of $(CTOA)^{F.G.}$ and $(CTOA)_R$ for deep notch test.